

Baryon number violating neutron decays to dark matter via the emission of a π^0 meson, η meson or photon



LUNDS
UNIVERSITET

Rutger Nieuwenhuis

Supervisors: Bernhard Meirose and Roman Pasechnik

Lund University

Department of Physics

Division of Particle and Nuclear Physics

Project Duration: 15 credits, 2 months full-time equivalent

Date of the examination: June, 2024

Thesis submitted for the degree of Bachelor of Science

Abstract

The existence of a baryon number violating process is one of Sakharov's conditions to explain the observed baryon asymmetry in the universe. The Standard Model is nearly symmetric with respect to the baryon number, and hence we are motivated to look for physics beyond the Standard Model. In this thesis, we consider an effective field theory operator that couples the neutron to a proposed dark fermion X , leading to decay channels containing mesons and photons. The unpolarized width for these decays is computed analytically. The model is subsequently implemented in `CalcHEP` via the definition of a new effective vertex. This allows for a Monte Carlo simulation of the three-body decay $n \rightarrow X + \gamma\gamma$, where the off-shell meson decays into a pair of photons. The narrow width of the mesons is seen in the invariant mass reconstruction of the photons in this channel. The case of a small mass gap between the neutron and the decay products is considered, where these channels are kinematically forbidden for bound neutrons in stable nuclei. We conclude that the analyzed decays are less experimentally constrained for free neutrons, and argue that searches for exotic neutron decays with a small mass gap could take place at the upcoming HIBEAM and NNBAR experiments at the European Spallation Source.

Popular Science Summary

Everything around us is made of matter, consisting of three fundamental building blocks: the positively charged proton, the negatively charged electron and the neutron without any charge. All types of matter have twins with opposite electric charge, called antimatter. The three fundamental building blocks of antimatter are the negatively charged antiproton, the positively charged positron and the neutral antineutron. When a matter and antimatter particle come together, they annihilate each other in a big burst of energy.

The current leading theory of particle physics, called the Standard Model, is nearly symmetric with respect to matter and antimatter. This means that every interaction allowed within the Standard Model creates nearly equal amounts of matter and antimatter. However, in everyday life we only encounter matter. After all, if there would be any antimatter around us, it would collide with the ordinary matter and annihilate into pure energy.

One of the current questions in physics is why there is so much matter, and so little antimatter in the universe. This observation has led physicists to speculate that there might be interactions beyond the Standard Model. These interactions would violate the matter-antimatter symmetry, allowing for a process that creates an excess of matter.

In this thesis, we consider such a process and analyze its consequences. Namely, we consider a model where the neutron decays to a new stable particle and an unstable particle, which can in turn decay to rays of energy. The new particle would not interact with particles in any other way, and hence it would create a different type of matter called dark matter.

This process would destroy a neutron, leading to matter disappearing instead of appearing. However, in the dense conditions of the early universe, the inverse of this process could occur frequently, leading to the creation of matter. In contrast, the process would be rare in the conditions of a laboratory. Many experiments have searched for such exotic neutron decays, putting very strict experimental limits on this model.

However, most of these experiments deal with *bound* neutrons, neutrons tied to other matter. If the difference between the mass of the neutron and the mass of the particles that it decays into is small, this decay cannot happen for bound neutrons. In contrast, the decay is possible for free neutrons.

The upcoming HIBEAM/NNBAR experiments at the European Spallation Source (ESS) analyze large amounts of free neutrons, and hence could observe this decay. In this thesis, we consider this case of a small mass difference and compute how rare the processes allowed by the model would be under this condition. Additionally, we run numerical simulations which allows us to see what it would be like to observe these interactions in experiments. We conclude that this model is a candidate for observation at HIBEAM/NNBAR and that the possibility of observing such exotic neutron decays should be further investigated.

Acknowledgements

I would like to extend my sincere gratitude to Bernhard Meirose for involving me in the HIBEAM/NNBAR collaboration from an early point in my Bachelor studies. Our conversations during our shared shifts at MAX IV have peaked my interest in particle physics, and without his initiative this project would not have taken off. Additionally, I would like to thank Roman Pasechnik, Hector Gisbert, Antonio Rodriguez, Luiz Henrique Vale Silva as well as Bernhard Meirose for the many interesting discussions, providing me with resources and helping me when I ran into problems. The topic of exotic neutron decays at HIBEAM/NNBAR is far from finished, and I hope that we can keep working together on this in the future.

Glossary of terms

SM - Standard Model

BSM - Beyond the Standard Model

\mathcal{B} - Baryon Number

ESS - European Spallation Source

Contents

1	Introduction	1
1.1	The mass gap and free neutrons	1
2	Theory and Methodology	2
2.1	The effective Lagrangian	2
2.2	The coupling of π^0 and η to photons	4
2.3	Kinematics of two-body decays	4
2.4	Summing over fermion spin states	5
2.5	The CalcHEP software	6
3	Results	6
3.1	Two-body decays	6
3.1.1	Decay with mesons	6
3.1.2	Decay with photons	9
3.2	Implementation in CalcHEP	10
3.2.1	The $n \rightarrow \phi + X$ vertex	10
3.2.2	The $\phi \rightarrow \gamma\gamma$ vertex	11
3.3	The $n \rightarrow X + \gamma\gamma$ decay	12
4	Summary and Outlook	15
	Appendices	17
	Appendix A CalcHEP tables	18
	Appendix B FeynCalc input for trace evaluation	19
	Bibliography	22

1. Introduction

The universe contains an observed asymmetry, with the amount of matter vastly exceeding the amount of antimatter. This asymmetry may be quantified by the concept of the baryon number \mathcal{B} . In the Standard Model (SM) framework, quarks are assigned $\mathcal{B} = \frac{1}{3}$ with all other particles having $\mathcal{B} = 0$. Consequently, baryons such as the proton and the neutron have $\mathcal{B} = 1$. Corresponding antiparticles carry a baryon number of the opposite sign.

The existence of a process that violates baryon number is required to explain the baryon asymmetry of the universe, as formulated by Sakharov [1]. However, the SM admits an accidental global symmetry, leading to \mathcal{B} being conserved as a Noether charge [2]. This symmetry only exists on a classical level, with non-perturbative quantum effects leading to baryon number violation within the Standard Model [3]. However, these effects are heavily suppressed at low temperatures. This has been proposed as a source of baryogenesis in the early universe [4], but it is also argued that it is insufficient to explain the amount of matter in the universe [5]. Hence, we are motivated to look for processes beyond the Standard Model (BSM).

In this thesis, we consider a baryon number violating process where the neutron n decays into a dark fermion X and SM particles. The term dark refers here to the absence of other interactions with the SM, leading to missing energy in particle detection. If no further interactions are postulated, such a fermion could also be a candidate for cosmological dark matter. We will analytically calculate the lifetime of such exotic decays as a function of the free parameters of the theory. Furthermore, we will also discuss the implementation of this model in the `CalcHEP` software [6] which can be used for extended phenomenology. Using `CalcHEP`, we will then analyze the three-body $n \rightarrow X + \gamma\gamma$ decay.

1.1 The mass gap and free neutrons

Large mass experiments such as Super-Kamiokande [7] have put strict experimental constraints on exotic neutron decays like the ones discussed in this thesis. These constraints will be even further improved by future experiments such as the Deep Underground Neutrino Experiment (DUNE) [8] and Hyper-Kamiokande [9].

However, these large mass experiments only deal with bound neutrons. When the total mass of the decay products is close to the neutron mass, bound neutrons in stable nuclei do not have sufficient energy available to escape their potential well. This is the mechanism that forbids β -decay for most bound neutrons. Free neutrons are not in a potential well, and hence they do have the possibility of β -decay.

This argument also extends to the case of exotic decays. Large mass experiments therefore have a blind spot in their phase space when the total mass of the final state particles is approximately equal to the neutron mass. However, since the mass of the dark fermion X is unknown, such decays can always be hypothesized. If the operator that would induce a small mass gap decay would also induce decays with a larger mass gap, one could further speculate that the coupling of

this operator falls off quickly at large momenta of the outgoing particles, as is the case for decays with a large mass gap.

This narrow area of the phase space can only be explored by experiments with free neutrons. The proposed HIBEAM [10] and NNBAR [11] experiment at the European Spallation Source (ESS) are potential candidates to explore this area. Although the amount of neutrons observed at large mass experiments exceeds the amount of neutrons observed at HIBEAM/NNBAR by several orders of magnitude, HIBEAM/NNBAR handles free neutrons.

This thesis is written with the HIBEAM/NNBAR experiments in mind, and as a source for future publications on the possibility of measuring exotic decays at HIBEAM/NNBAR. We will therefore also consider the case of a small mass gap for the decays analyzed in this thesis.

2. Theory and Methodology

This chapter discusses the effective Lagrangian under consideration, as well as the theoretical framework used to calculate an unpolarized decay width Γ (and lifetime $\tau = \hbar/\Gamma$) from a Feynman amplitude \mathcal{M} . A brief overview of vertex implementation in the `CalcHEP` software is also given. Throughout this thesis, we will work in natural units such that $\hbar = c = 1$.

2.1 The effective Lagrangian

In this thesis, we postulate an effective field theory operator that violates baryon number conservation by one unit

$$\frac{(Xudd)_R}{M^2} \quad (2.1)$$

where X is a stable new dark fermion field and u, d denote the fields of the up- and down-quark, respectively. All fields involved have right-handed chirality, as denoted by the subscript R . The constant $M \gg 1$ TeV is the unknown new physics scale. As we only postulate a single operator, any coupling constant is absorbed in the definition of M [12, 13].

This effective field theory operator couples the right-handed neutron $P_R n = \frac{1}{2}(1 + \gamma^5)n$ to the dark fermion and the π^0 and η meson fields. The Lagrangian governing this interaction is

$$\mathcal{L} = \bar{X}^c (C_{\text{mix}} + iC_{X\pi^0}\pi^0 + iC_{X\eta}\eta) P_R n. \quad (2.2)$$

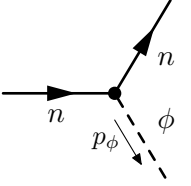
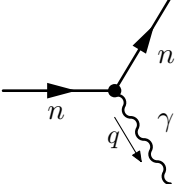
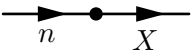
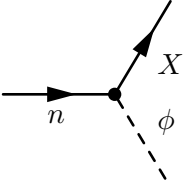
which naturally also violates baryon number conservation by one unit [13, 14]. Here, C denote real constants that we define below. Notice that this Lagrangian allows right-handed neutrons to mix with the dark fermion, but we have not assumed that the dark fermion mass is equal to the neutron mass. Hence, this mixing only occurs via off-shell neutrons.

Additionally, we may add a Lagrangian that couples the neutron to the π^0 and η meson fields, as well as the photon field A_μ with four-momentum q via the magnetic dipole moment of the neutron. In contrast to equation (2.2), this Lagrangian conserves the baryon number. It is given by

$$\mathcal{L} = (C_{n\pi^0}\partial_\mu\pi^0 + C_{n\eta}\partial_\mu\eta)\bar{n}\gamma^\mu\gamma^5 n + iC_{n\gamma}\bar{n}\sigma^{\mu\nu}q_\nu F_2(q^2)nA_\mu \quad (2.3)$$

where $F_2(q^2)$ is a form factor [13]. If the photon is created on-shell, then $q^2 = 0$ and $F_2(0) = -1.9130427(5)$, the magnetic moment of the neutron [15]. Together, these terms give rise to the Feynman rules displayed in table 2.1.

Table 2.1: Feynman rules for the Lagrangians in equations (2.2) and (2.3) ($\phi = \pi^0, \eta$).

Vertex	Factor
	$-C_{n\phi}\not{p}_\phi\gamma^5$
	$-C_{n\gamma}\sigma^{\mu\nu}q_\nu F_2(q^2)$
	$iC_{\text{mix}}P_R$
	$-C_{X\phi}P_R$

In equations (2.2) and (2.3), we have defined the constants

$$C_{n\pi^0} \equiv -\frac{D+F}{2f_\pi} \quad (2.4)$$

$$C_{n\eta} \equiv \frac{3F-D}{2\sqrt{3}f_\pi} \quad (2.5)$$

$$C_{n\gamma} \equiv \frac{\sqrt{\pi\alpha}}{m_p} \quad (2.6)$$

$$C_{\text{mix}} \equiv \frac{\beta}{M^2} \quad (2.7)$$

$$C_{X\pi^0} \equiv \frac{\beta}{2f_\pi M^2} \quad (2.8)$$

$$C_{X\eta} \equiv -\frac{\sqrt{3}\beta}{2f_\pi M^2} \quad (2.9)$$

where $D = 0.80(1)$, $F = 0.47(1)$, $\beta = 0.0120(26) \text{ GeV}^3$ are parameters determined via lattice

QCD methods [16], $f_\pi \approx 130.2(8) \text{ MeV}/\sqrt{2}$ is the pion decay constant [15], α is the fine-structure constant and m_p is the proton mass. Notice that in this framework, the only undetermined parameters are the mass of the dark fermion m_X and the new physics scale M .

2.2 The coupling of π^0 and η to photons

The π^0 and η mesons are unstable particles, which can decay into a state containing two photons. The branching ratio for this decay is approximately 98.823(34) % and 39.36(18) %, respectively [15]. These photons are a good candidate for detection, as they have a relatively high momentum of $m_\phi/2$ in the rest frame of the meson.

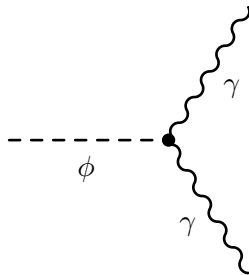


Figure 2.1: The effective vertex of a meson $\phi = \pi^0, \eta$ decaying into two photons.

The decay of the π^0 and η mesons into two photons is governed by relevant terms of the Wess-Zumino-Witten Lagrangian

$$\mathcal{L}_{\text{WZW}} = -\frac{\alpha}{8\pi f_\pi} \epsilon_{\mu\nu\sigma\rho} F^{\mu\nu} F^{\sigma\rho} (\pi^0 + \frac{1}{\sqrt{3}} \eta_8) \quad (2.10)$$

where $\epsilon_{\mu\nu\sigma\rho}$ denotes the Levi-Civita symbol and $F^{\mu\nu}$ is the electromagnetic field strength tensor [17]. Expanding the field strength tensors and rearranging the indices according to the Levi-Civita symbol, we obtain

$$\mathcal{L}_{\text{WZW}} = \frac{\alpha}{2\pi f_\pi} \epsilon_{\mu\nu\sigma\rho} (i\partial^\mu A^\nu)(i\partial^\sigma A^\rho) (\pi^0 + \frac{1}{\sqrt{3}} \eta_8). \quad (2.11)$$

The physical η meson is a combination of the η_8 and η_1 eigenstates

$$\eta = \eta_8 \cos \theta - \eta_1 \sin \theta \quad (2.12)$$

with a mixing angle θ . The term in the Lagrangian can be multiplied by a factor to compensate for this, which can be derived from $\eta - \eta'$ mixing and fitted to experimental data [18, 19]. For our present purposes, it suffices to approximate this factor as $\sqrt{3}$ and simply replace $\eta_8/\sqrt{3} \rightarrow \eta$.

2.3 Kinematics of two-body decays

Using the Feynman rules, the invariant amplitude \mathcal{M} for a given process can be computed via a set of Feynman diagrams. The width integrated over the angular distribution for a two-body decay of a particle of mass M as a function of $|\mathcal{M}|^2$ is given by

$$\Gamma = \frac{|\mathbf{p}|}{8\pi M^2} |\mathcal{M}|^2 \quad (2.13)$$

where \mathbf{p} is the three-momentum of one of the decay products in the rest frame of the decaying particle. By conservation of four-momentum, $|\mathbf{p}|$ may be expressed as

$$|\mathbf{p}| = \frac{1}{2M} \sqrt{\lambda(M^2, m_1^2, m_2^2)} \quad (2.14)$$

where m_1 and m_2 are the masses of the decay products and $\lambda(x, y, z) = x^2 + y^2 + z^2 - 2xy - 2xz - 2yz$ is the Källén function [15].

Furthermore, conservation of four-momentum also implies that

$$M^2 = p_M^2 = (p_1 + p_2)^2 = m_1^2 + m_2^2 + 2(p_1 \cdot p_2) \quad (2.15)$$

$$m_1^2 = p_1^2 = (p_M - p_2)^2 = m_1^2 + m_2^2 - 2(p_M \cdot p_2) \quad (2.16)$$

$$m_2^2 = p_2^2 = (p_M - p_1)^2 = m_1^2 + m_2^2 - 2(p_M \cdot p_1) \quad (2.17)$$

where p_M denotes the four-momentum of the particle of mass M and p_1, p_2 denote the four-momenta of the particles with mass m_1 and m_2 , respectively. Hence we see that all products of four-momenta can be expressed in terms of the invariant masses of the involved particles.

2.4 Summing over fermion spin states

The Feynman amplitude \mathcal{M} assumes that the spin states of the incoming and outgoing particles are known. This leads to the decay width of a polarized process. In practise, the involved particles are often unpolarized. Hence, we wish to average over the spin states of the initial state particles and sum over the spin states of the final particles.

Suppose that $\mathcal{M} \sim [\bar{s}_a \Gamma s_b]$, where $s_a = u_a, v_a$ is a spinor of a particle a with mass m_a and four-momentum p_a . Here u_a (v_a) denotes the spinor of an (anti)fermion. Then for any 4×4 matrix Γ ,

$$\sum_{\text{spins}} |\mathcal{M}|^2 \sim \sum_{\text{spins}} [\bar{s}_a \Gamma s_b] [\bar{s}_a \Gamma s_b]^* = \text{Tr}[\Gamma (\sum_{\text{spins}} s_b \bar{s}_b) \bar{\Gamma} (\sum_{\text{spins}} s_a \bar{s}_a)] \quad (2.18)$$

where $\bar{\Gamma} \equiv \gamma^0 \Gamma^\dagger \gamma^0$. For ordinary spinors, we have

$$\sum_{\text{spins}} s_a \bar{s}_a = \not{p}_a \pm m_a \quad (2.19)$$

where the mass term is positive when $s_a = u_a$, and negative when $s_a = v_a$ [20].

Suppose that instead of an ordinary spinor s , we have the charge conjugated spinor $s^c = C \bar{s}^T$, where $C = i\gamma^2 \gamma^0$ is the charge conjugation matrix. It satisfies the properties [21]

$$C \gamma^\mu = -(\gamma^\mu)^T C \quad (2.20)$$

$$C = -C^{-1} = -C^\dagger = -C^T. \quad (2.21)$$

We also note that

$$\bar{s}^c = (s^c)^\dagger \gamma^0 = (C \bar{s}^T)^\dagger \gamma^0 = -s^T C^\dagger. \quad (2.22)$$

For the spin sum in equation (2.19), we then obtain

$$\begin{aligned} \sum_{\text{spins}} s_a^c \bar{s}_a^c &= - \sum_{\text{spins}} C \bar{s}_a^T s_a^T C^\dagger = - \sum_{\text{spins}} C (s_a \bar{s}_a)^T C^\dagger \\ &= -C (\not{p}_a \pm m_a)^T C^\dagger = -C ((\gamma^\mu)^T (p_a)_\mu \pm m_a) C^\dagger = \not{p}_a \mp m_a. \end{aligned} \quad (2.23)$$

We see that if the spinor is charge-conjugated, the mass term changes sign in comparison with equation (2.19).

2.5 The CalcHEP software

In order to do extended phenomenology, it is beneficial to implement the model in the CalcHEP software. CalcHEP allows for the automatic calculation of cross sections and decay widths, as well as Monte Carlo event simulation [6]. Furthermore, the generated events can subsequently be used as input to detector simulations such as Geant4 [22–24].

To implement a model governed by a Lagrangian \mathcal{L} in CalcHEP, one takes the functional derivative of the action

$$S = \int \mathcal{L} dx^4 \quad (2.24)$$

in momentum-space with respect to the fields involved. The resulting expression has a prefactor in the form of a (potentially complex) scalar, and a Lorentz factor comprising of tensor expressions and the γ -matrices. These two components, as well as the fields involved, are entered into a table in CalcHEP.

Note that for this functional derivative, CalcHEP works directly with the charge conjugated fields, not the Dirac conjugated fields. The functional derivatives for these fields relate to each other via [6]

$$\frac{\delta}{\delta\psi^c} = (C^{-1})^T \frac{\delta}{\delta\bar{\psi}}. \quad (2.25)$$

The momentum-conserving δ -function and the $(C^{-1})^T$ term are implied in CalcHEP and do not need to be entered explicitly [6]. All CalcHEP tables used in this thesis will be listed in appendix A.

3. Results

This chapter covers the results obtained in this thesis. First, the width of the two-body decays enabled by the Lagrangians in equations (2.2) and (2.3) is computed analytically. Then, the implementation of these Lagrangians in CalcHEP is discussed, which is used to analyze the $n \rightarrow X + \gamma\gamma$ decay channel.

3.1 Two-body decays

The Feynman rules outlined in table (2.1) give rise to the neutron decaying to a dark fermion with a photon or a meson in the final state. In this section, we calculate the widths for these two-body decay channels in the case of unpolarized particles.

3.1.1 Decay with mesons

For the decay $n \rightarrow \phi + X$ ($\phi = \pi^0, \eta$), there is one contribution without mixing and one contribution with mixing. These are depicted in figures 3.1a and 3.1b, respectively. The Feynman amplitudes for these diagrams are given by

$$\mathcal{M}_{\text{nomix}} = -iC_{X\phi}\bar{v}_X^c P_R u_n \quad (3.1)$$

$$\mathcal{M}_{\text{mix}} = iC_{\text{mix}}C_{n\phi}\bar{v}_X^c P_R \frac{\not{p}_X + m_n}{m_X^2 - m_n^2} \not{p}_\phi \gamma^5 u_n \quad (3.2)$$

where we have used that the four-momentum of the off-shell neutron in the mixing diagram must be equal to the four-momentum of the outgoing dark fermion by momentum conservation.

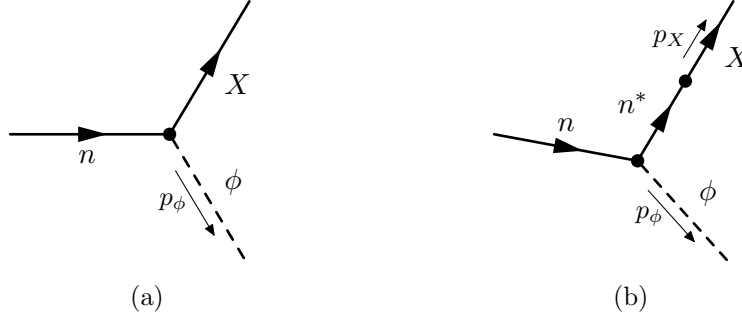


Figure 3.1: Feynman diagrams of the two-body decay of the neutron n to a dark fermion X and a meson $\phi = \pi^0, \eta$, (a) without mixing (b) with mixing of an off-shell neutron n^* to the dark fermion.

Using equations (2.18), (2.19) and (2.23) we can sum over the spin states of the total amplitude

$$\sum_{\text{spins}} |\mathcal{M}|^2 = \sum_{\text{spins}} |\mathcal{M}_{\text{nomix}} + \mathcal{M}_{\text{mix}}|^2 = \text{Tr}[\mathcal{A}(\not{p}_n + m_n)\gamma^0\mathcal{A}^\dagger\gamma^0(\not{p}_X + m_X)] \quad (3.3)$$

where we have defined the 4×4 matrix

$$\mathcal{A} \equiv -iC_{X\phi}P_R + \frac{iC_{\text{mix}}C_{n\phi}}{m_X^2 - m_n^2}(P_R(\not{p}_X + m_X)\not{p}_\phi\gamma^5). \quad (3.4)$$

Using that γ^5 is hermitian and anticommutes with the other γ -matrices, we compute

$$\gamma^0\mathcal{A}^\dagger\gamma^0 = iC_{X\phi}P_L + \frac{iC_{\text{mix}}C_{n\phi}}{m_X^2 - m_n^2}(\gamma^5\not{p}_\phi(\not{p}_X + m_X)P_L) \quad (3.5)$$

where $P_L = \frac{1}{2}(1 - \gamma^5)$.

With the use of the `FeynCalc` software in `Mathematica` [25–27], the trace of equation (3.3) can be evaluated. The input to `FeynCalc` for this is given in appendix B. After simplifying with four-momentum conservation, one obtains

$$\begin{aligned} \sum_{\text{spins}} |\mathcal{M}|^2 = & \frac{1}{(m_n^2 - m_X^2)} (-2C_{\text{mix}}C_{n\phi}C_{X\phi}(-m_n^4(3m_X^2 + m_\phi^2) + 3m_n^2m_X^4 + m_n^6 \\ & + m_X^4m_\phi^2 - m_X^6) + C_{\text{mix}}^2C_{n\phi}^2(-m_n^4(m_X^2 + m_\phi^2) - m_n^2(6m_X^2m_\phi^2 + m_X^4) \\ & + m_n^6 - m_X^4m_\phi^2 + m_X^6) + C_{X\phi}^2(m_n^2 - m_X^2)^2(m_n^2 + m_X^2 - m_\phi^2)). \end{aligned} \quad (3.6)$$

Note that we wish to average, not sum, over the spin states of the incoming neutron. Hence we multiply by a factor $\frac{1}{2}$ and use equations (2.13), (2.14) and (3.6) to obtain the decay width

$$\begin{aligned} \Gamma(n \rightarrow \phi + X) = & \frac{1}{32\pi m_n^3(m_n^2 - m_X^2)^2} \sqrt{-2m_n^2(m_X^2 + m_\phi^2) + m_n^4 + (m_X^2 - m_\phi^2)^2} \\ & (-2C_{\text{mix}}C_{n\phi}C_{X\phi}(-m_n^4(3m_X^2 + m_\phi^2) + 3m_n^2m_X^4 + m_n^6 + m_X^4m_\phi^2 - m_X^6) \\ & + C_{\text{mix}}^2C_{n\phi}^2(-m_n^4(m_X^2 + m_\phi^2) - m_n^2(6m_X^2m_\phi^2 + m_X^4) + m_n^6 - m_X^4m_\phi^2 + m_X^6) \\ & + C_{X\phi}^2(m_n^2 - m_X^2)^2(m_n^2 + m_X^2 - m_\phi^2)) \end{aligned} \quad (3.7)$$

where it is implied that if $m_\phi + m_X > m_n$, $\Gamma(n \rightarrow \phi + X) = 0$ due to the fact that the mass of the final state of a particle decay cannot exceed the mass of the original particle by momentum conservation.

For $M = 10^{15}$ GeV, the width and corresponding lifetime as a function of the dark fermion

mass are displayed in figures 3.2a and 3.2b, respectively. The propagation of the uncertainties in the involved constants from section 2.1 is shown by the shaded region in figure 3.2b. The kink in the graph is where $m_\eta + m_X = m_n$, and the decay channel with the η meson becomes disallowed. The results derived here match with the results of reference [13].

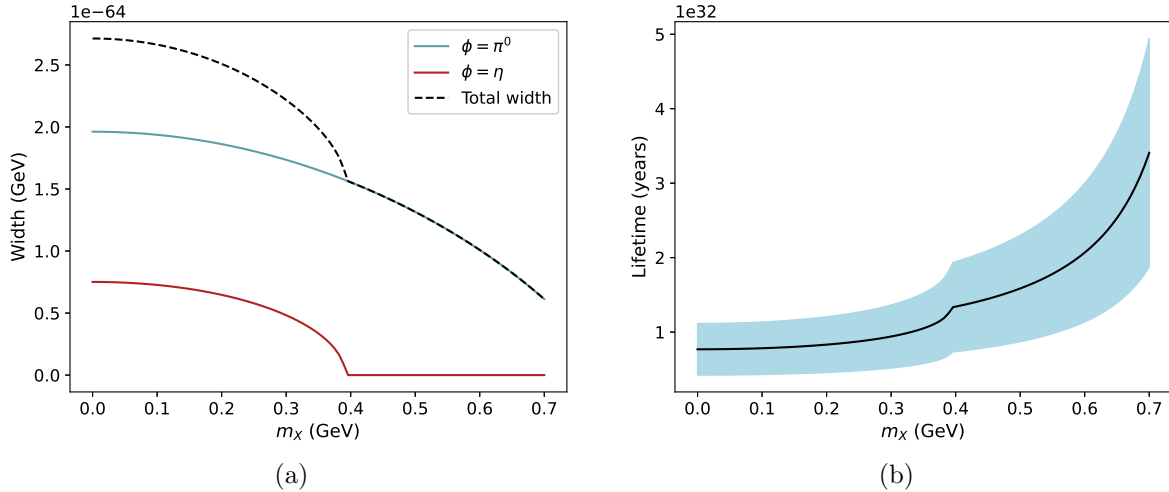


Figure 3.2: (a) Decay width and (b) total lifetime of the $n \rightarrow \phi + X$ ($\phi = \pi^0, \eta$) decay for the new physics scale $M = 10^{15}$ GeV. The shaded region in (b) corresponds to the propagated uncertainties from the involved constants. At the kink in the graph, the decay channel to an η meson becomes disallowed due to the total mass of the final state particles exceeding the neutron mass.

To simulate the small mass gap scenario, we may fix $m_X = m_p + m_e - m_\phi$, where m_e is the electron mass. This creates a mass gap similar to that of ordinary β -decay. In this case, equation (3.7) is a function of M alone and $\Gamma(n \rightarrow \phi + X) \propto M^{-4}$. The lifetime as a function of M is displayed in figure 3.3.

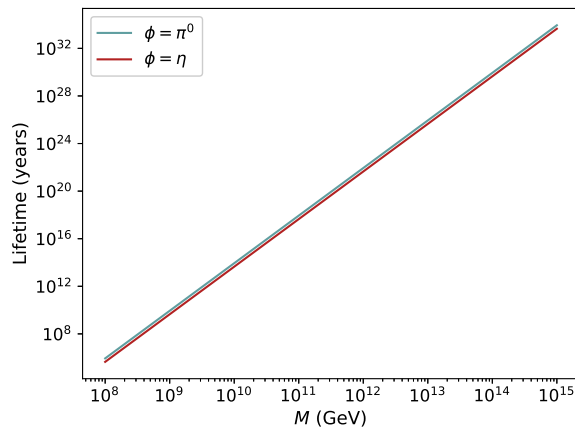


Figure 3.3: Lifetime of the $n \rightarrow \phi + X$ ($\phi = \pi^0, \eta$) decay as a function of the new physics scale M for a mass gap similar to that of β -decay ($m_X = m_p + m_e - m_\phi$).

3.1.2 Decay with photons

The relevant diagram for the $n \rightarrow \gamma + X$ decay is depicted in figure 3.4. The Feynman amplitude for this process is given by

$$\mathcal{M} = iC_{\text{mix}}C_{n\gamma}\bar{v}_X^c P_R \frac{\not{p}_X + m_n}{m_X^2 - m_n^2} \sigma^{\mu\nu} q_\nu F_2(0) u_n \epsilon_\mu^* \quad (3.8)$$

where ϵ_μ denotes the polarization state of the photon with four-momentum q .

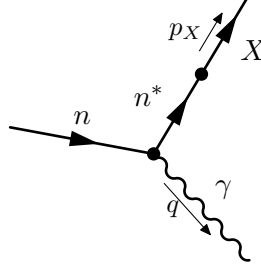


Figure 3.4: Feynman diagram of the two-body decay of the neutron to a dark fermion X and a photon.

When summed over, the polarization states satisfy the replacement [20]

$$\sum_{\text{polarizations}} \epsilon_\mu^* \epsilon_\nu \rightarrow -g_{\mu\nu}. \quad (3.9)$$

With equations (2.18), (2.19) and (2.23) we therefore obtain

$$\sum_{\text{spins}} \sum_{\text{polarizations}} |\mathcal{M}|^2 = \sum_{\text{polarizations}} \frac{C_{\text{mix}}^2 C_{n\gamma}^2 F_2(0)^2}{(m_X^2 - m_n^2)^2} \text{Tr}[\mathcal{A}^\alpha \epsilon_\alpha^* (\not{p}_n + m_n) \gamma^0 (\mathcal{A}^\beta)^\dagger \gamma^0 \epsilon_\beta (\not{p}_X + m_X)] \quad (3.10)$$

$$= -\frac{C_{\text{mix}}^2 C_{n\gamma}^2 F_2(0)^2}{(m_X^2 - m_n^2)^2} \text{Tr}[\mathcal{A}_\beta (\not{p}_n + m_n) \gamma^0 (\mathcal{A}^\beta)^\dagger \gamma^0 (\not{p}_X + m_X)] \quad (3.11)$$

where we have defined

$$\mathcal{A}^\mu \equiv iP_R (\not{p}_X + m_n) \sigma^{\mu\nu} q_\nu. \quad (3.12)$$

Using that $(\sigma^{\mu\nu})^\dagger = \gamma^0 \sigma^{\mu\nu} \gamma^0$, we find

$$\gamma^0 (\mathcal{A}^\mu)^\dagger \gamma^0 = -i\sigma^{\mu\nu} q_\nu (\not{p}_X + m_n) P_L \quad (3.13)$$

which allows us to evaluate this trace with `FeynCalc` to obtain

$$\sum_{\text{spins}} \sum_{\text{polarizations}} |\mathcal{M}|^2 = 2F_2(0)^2 C_{\text{mix}}^2 C_{n\gamma}^2 (m_n^2 + m_X^2). \quad (3.14)$$

The `FeynCalc` input used can be found in appendix B.

Note that the on-shell photon has no mass, so equation 2.14 simplifies to

$$|\mathbf{p}| = \frac{1}{2m_n} (m_n^2 - m_X^2). \quad (3.15)$$

Multiplying equation (2.13) by $\frac{1}{2}$ to average over the spin states of the incoming neutron, we obtain the decay width for the channel containing a photon

$$\Gamma(n \rightarrow \gamma + X) = \frac{C_{\text{mix}}^2 C_{n\gamma}^2 F_2(0)^2}{16\pi m_n^3} (m_n^4 - m_X^4). \quad (3.16)$$

The lifetime of this decay as a function of m_X when $M = 10^{15}$ GeV is shown in figure 3.5a. The propagation of the uncertainties in the physical constants from section 2.1 is shown by the shaded region in this figure. The obtained expression matches the results of reference [13]. The lifetime of this decay as a function of M for the case of a mass gap similar to that of β -decay with $m_X = m_p + m_e$ is displayed in figure 3.5b. Note that $\Gamma(n \rightarrow \gamma + X) \propto M^{-4}$.

The lifetime of the $n \rightarrow \gamma + X$ is roughly 10^3 years longer than the lifetime of the $n \rightarrow \phi + X$ decay. Additionally, in the case of a small mass gap, the photon will have a very low momentum and thus be hard to detect. Hence we focus on the $n \rightarrow \phi + X$ channel in the rest of this thesis.

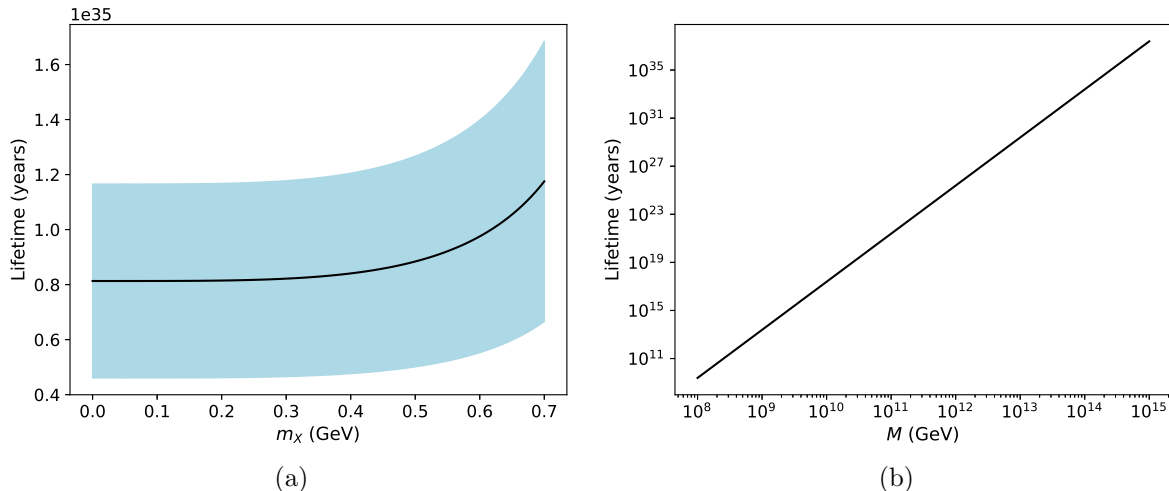


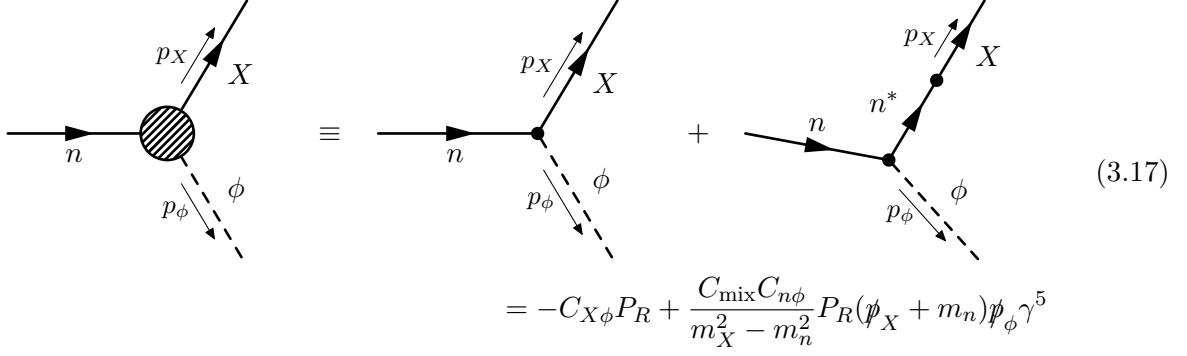
Figure 3.5: Lifetime of the $n \rightarrow \gamma + X$ decay (a) at the new physics scale $M = 10^{15}$ GeV as a function of m_X and (b) as a function of the new physics scale M for the case of a mass gap similar to that of β -decay ($m_X = m_p + m_e$). The shaded region corresponds to the propagated uncertainties from the involved constants.

3.2 Implementation in CalcHEP

This section discusses the implementation of the $n \rightarrow \phi + X$ and $\phi \rightarrow \gamma\gamma$ vertex in CalcHEP. These vertices will be used to analyze the $n \rightarrow X + \gamma\gamma$ decay.

3.2.1 The $n \rightarrow \phi + X$ vertex

The Lagrangian in equation (2.2) contains a term which mixes the neutron to the dark fermion. Such a two-particle vertex is not allowed in CalcHEP. However, since we do not assume that $m_X = m_n$, the mixing term is only relevant for off-shell neutrons. Hence we define the effective vertex



$$\begin{aligned}
& \text{Diagram 1} \equiv \text{Diagram 2} + \text{Diagram 3} \\
& = -C_{X\phi}P_R + \frac{C_{\text{mix}}C_{n\phi}}{m_X^2 - m_n^2}P_R(\not{p}_X + m_n)\not{p}_\phi\gamma^5
\end{aligned} \tag{3.17}$$

which is a three-particle vertex that includes both the mixing and no-mixing contributions. The Lagrangian corresponding to this effective vertex is given by

$$\mathcal{L}_{\text{eff}} = \bar{X}^c \left(iC_{X\phi}P_R - i\frac{C_{\text{mix}}C_{n\phi}}{m_X^2 - m_n^2}P_R(\gamma^\mu(i\overleftarrow{\partial}_\mu) + m_n)\gamma^\nu(i\partial_\nu\phi)\gamma^5 \right) n \tag{3.18}$$

where $\overleftarrow{\partial}$ denotes the four-derivative acting on the fermion field to the left.

Besides the vertex given above, **CalcHEP** also requires the conjugate vertex. Hence we compute the hermitian conjugate of equation (3.18)

$$\begin{aligned}
\mathcal{L}_{\text{eff}}^\dagger &= n^\dagger \left(-iC_{X\phi}P_R + i\frac{C_{\text{mix}}C_{n\phi}}{m_X^2 - m_n^2}\gamma^5(-i\partial_\nu\phi)\gamma^0\gamma^\nu\gamma^0(\gamma^0\gamma^\mu\gamma^0(-i\overrightarrow{\partial}_\mu) + m_n)P_R \right) \gamma^0 X^c \\
&= \bar{n} \left(-iC_{X\phi}P_L - i\frac{C_{\text{mix}}C_{n\phi}}{m_X^2 - m_n^2}\gamma^5(-i\partial_\nu\phi)\gamma^\nu(\gamma^\mu(-i\overrightarrow{\partial}_\mu) + m_n)P_L \right) X^c
\end{aligned} \tag{3.19}$$

where $\overrightarrow{\partial}$ denotes the four-derivative acting on the fermion field to the right.

The relevant functional derivatives for the action

$$S_{\text{eff}} = \int \mathcal{L}_{\text{eff}} + \mathcal{L}_{\text{eff}}^\dagger dx^4 \tag{3.20}$$

are then given by

$$\frac{\delta S_{\text{eff}}}{\delta X \delta n \delta \phi} = \frac{\delta S_{\text{eff}}}{\delta (X^c)^c \delta n \delta \phi} = (C^{-1})^T \frac{\delta S_{\text{eff}}}{\delta \bar{X}^c \delta n \delta \phi} \tag{3.21}$$

and

$$\frac{\delta S_{\text{eff}}}{\delta n^c \delta X^c \delta \phi} = (C^{-1})^T \frac{\delta S_{\text{eff}}}{\delta \bar{n} \delta X^c \delta \phi} \tag{3.22}$$

where we have used equation (2.25). Additionally, in **CalcHEP** the momentum is taken to go in to the vertex, whereas we have derived the Feynman rules for momenta going out of the vertex. Hence we flip the sign of all momenta when implementing the vertices in **CalcHEP**. The full **CalcHEP** tables with these vertices are given in appendix A.

For two-body decays such as $n \rightarrow \phi + X$, **CalcHEP** computes the decay width analytically [6]. The total width for $M = 10^{15}$ GeV as computed by **CalcHEP** is displayed in figure 3.6. The results match the analytical calculation done in section 3.1.

3.2.2 The $\phi \rightarrow \gamma\gamma$ vertex

The Lagrangian given by equation (2.11) can be directly implemented in **CalcHEP**. This vertex is also given in the tables in appendix A. Note that we multiply the vertex by a symmetry factor of 2 due to the two identical photons. With this vertex, **CalcHEP** computes a π^0 width of 7.78 eV and

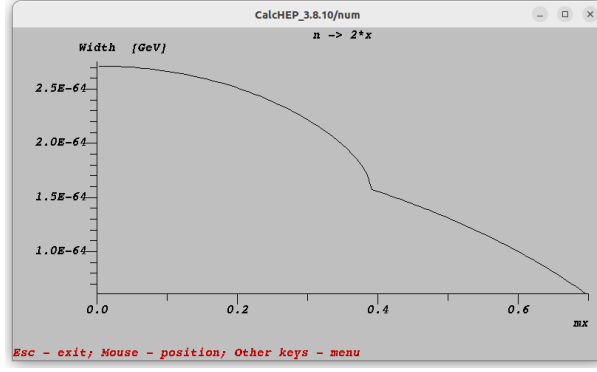


Figure 3.6: Decay width of $n \rightarrow \phi + X$ ($\phi = \pi^0, \eta$) as a function of m_X at $M = 10^{15}$ GeV, generated by CalcHEP.

a η width of 520 eV. This compares well to the experimental values of

$$\Gamma(\pi^0 \rightarrow \gamma\gamma) = \frac{\hbar}{8.43(13) \times 10^{-17} \text{ s}} \cdot 98.823(34) \% = 7.72(12) \text{ eV}$$

and $\Gamma(\eta \rightarrow \gamma\gamma) = 516(18) \text{ eV}$ [15]. Note that since this is a two-body decay, CalcHEP does this calculation analytically.

3.3 The $n \rightarrow X + \gamma\gamma$ decay

Using the implemented model, a Monte Carlo simulation can be run in CalcHEP for the $n \rightarrow X + \gamma\gamma$ decay. The two contributing diagrams for this process are displayed in figure 3.7. The data displayed in this section is an average of 40 Monte Carlo sessions with 1000000 events per session for 8 distinct values of m_X .

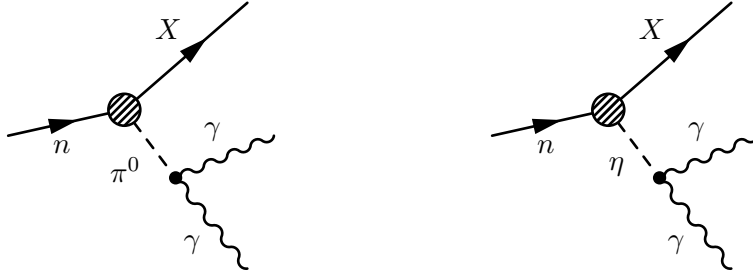


Figure 3.7: Feynman diagrams for the three-body decay of the neutron n to a dark fermion X and a pair of photons $\gamma\gamma$. The process can occur via an off-shell π^0 or η meson.

The width of this decay at $M = 10^{15}$ GeV as a function of m_X is displayed in figure 3.8, as well as the width of the $n \rightarrow X + \phi$ decay computed analytically in section 3.1. The values match closely, which can be attributed to the short lifetime (i.e. narrow width) of the η and π^0 meson. This means that the mesons are created mostly close to the mass shell, and the process is similar to that of the meson being created fully on-shell in the $n \rightarrow X + \phi$ process.

The fact that the mesons are created close to on-shell can be confirmed by performing an invariant mass reconstruction with the momenta of the two photons. If two photons with momenta q_1 and q_2 originate from the decay of a single particle of mass m and momentum p , four-momentum conservation allows m to be expressed in terms of the photon momenta

$$m = \sqrt{p^2} = \sqrt{(q_1 + q_2)^2}. \quad (3.23)$$

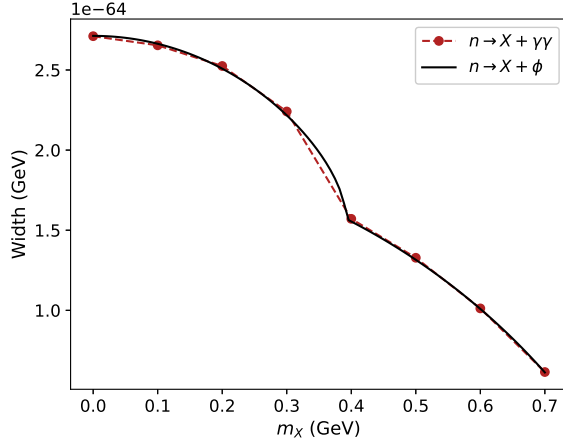


Figure 3.8: The width of the $n \rightarrow X + \gamma\gamma$ decay as computed in a Monte Carlo simulation in `CalcHEP` compared to the width of the $n \rightarrow X + \phi$ ($\phi = \eta, \pi^0$) decay computed analytically. The new physics scale is set to $M = 10^{15}$ GeV.

The invariant mass reconstruction of the photons in the Monte Carlo simulation for $m_X = 0.2$ GeV and $M = 10^{15}$ GeV is displayed in figure 3.9. The normalization in this graph is so that the total area under the curve integrates to the total width of the process. The graph is indeed the shape of two narrow Breit-Wigner distributions with sharp peaks at m_{π^0} and m_η .

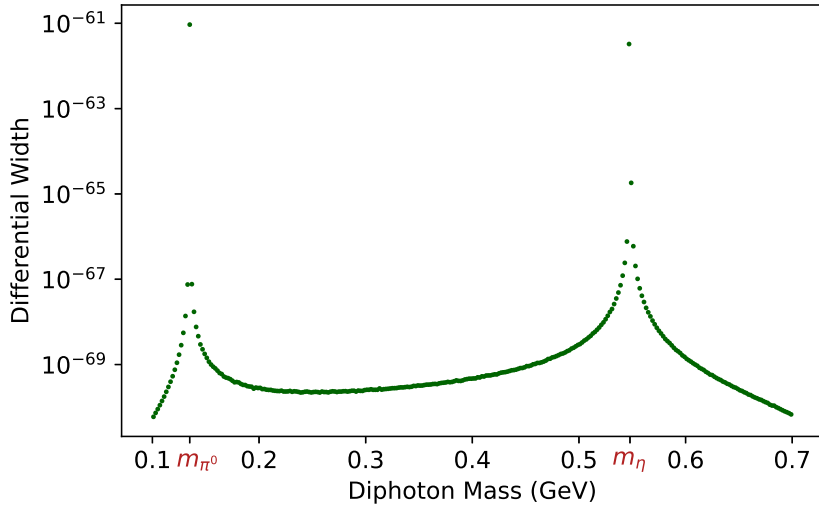


Figure 3.9: Diphoton mass of the $n \rightarrow X + \gamma\gamma$ decay at $m_X = 0.2$ GeV and a new physics scale of $M = 10^{15}$ GeV.

In the case of a small mass gap equivalent to that of β -decay ($m_X = m_p + m_e - m_\phi$), only the respective process with the off-shell ϕ can occur. The other meson would have to be too far off-shell to make significant contributions to the decay width. The lifetime as a function of the cutoff scale for the small mass gap case is displayed in figure 3.10. The results closely match those

of the $n \rightarrow \phi + X$ decay displayed in figure 3.3 due to the narrow width of the mesons. The invariant mass reconstruction of the two photons in the small mass gap case is displayed in figure 3.11.

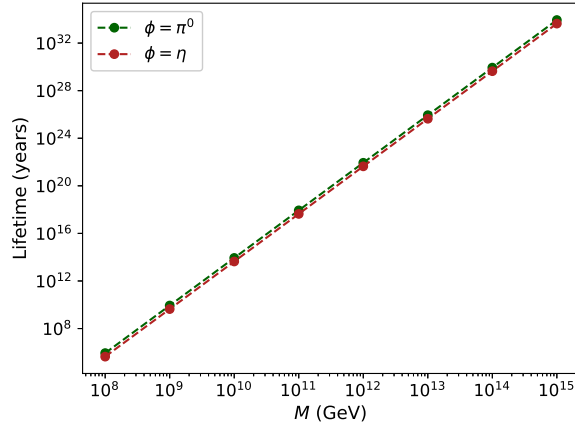


Figure 3.10: Lifetime of the $n \rightarrow X + \gamma\gamma$ decay via an off-shell meson ϕ with $m_X = m_p + m_e - m_\phi$ as a function of the new physics scale M .

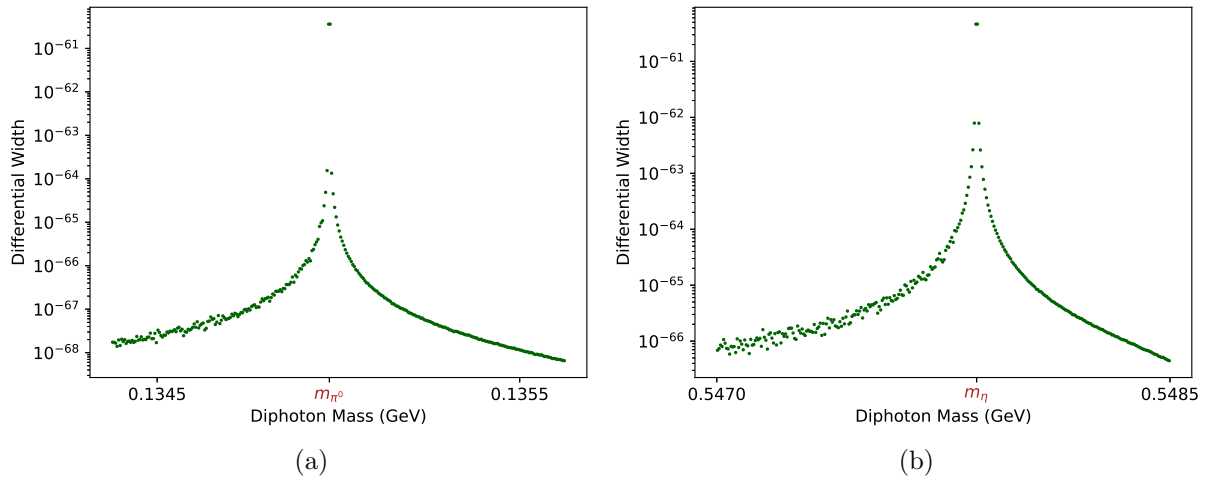


Figure 3.11: Diphoton mass of the $n \rightarrow X + \gamma\gamma$ decay via an off-shell meson ϕ with $m_X = m_p + m_e - m_\phi$ at a new physics scale $M = 10^{15}$ GeV, (a) $\phi = \pi^0$ (b) $\phi = \eta$.

By implementing the neutron coupling to the π^0 and η mesons via the Lagrangian in equation (2.3) in `CalcHEP`, decay channels with multiple photon pairs can be analyzed. An example of such a decay channel is depicted in figure 3.12. These `CalcHEP` vertices are also given in the tables in appendix A.

For every meson ϕ emitted by the neutron before decaying, an additional pair of photons is created (ignoring other decay channels of ϕ). To ensure a small mass gap, the mass of X is given by

$$m_X = m_p + m_e - \sum_i m_{\phi_i} \quad (3.24)$$

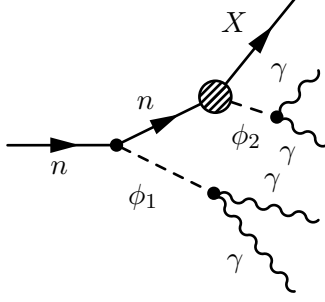


Figure 3.12: A Feynman diagrams for the $n \rightarrow X + 4\gamma$ decay via two off-shell mesons ϕ_1 and ϕ_2 ($\phi = \pi^0, \eta$).

where we sum over all emitted mesons. With `CalcHEP`, the relevant diagrams for these cases can be selected and the width can be computed via a Monte Carlo simulation. We compute the width for two photon pair production over 40 sessions with 100000 events per session.

As seen before, $\Gamma \propto \frac{1}{M^4}$. We hence compute the average of $M^4\Gamma$ for different values of M . For two photon pairs, we use four values of M from 10^9 GeV to 10^{15} GeV. For one photon pair, the same data as in figure 3.10 is used. The result for one and for two produced photon pairs is displayed in table 3.12. Since the integration errors are of the order of a few percent, they are discarded. We see that the production of two photon pairs is significantly rarer than the production of a single photon pair.

Table 3.1: The possible meson combinations for one or two produced photon pairs, as well as the mass of the X particle to ensure a small mass gap. The width Γ is computed via a Monte Carlo simulation for different values of the new physics scale M . The standard deviation of $M^4\Gamma$ is denoted by σ .

Photon pairs	mesons	m_X (GeV)	$M^4\Gamma$ (GeV ⁵)	σ (GeV ⁵)
1	π^0	0.8038	2.416×10^{-6}	2.793×10^{-9}
	η	0.3909	4.798×10^{-6}	2.404×10^{-9}
2	$2\pi^0$	0.6688	2.192×10^{-14}	3.533×10^{-17}
	π^0, η	0.2559	1.150×10^{-12}	2.379×10^{-14}

In the `CalcHEP` simulations, we have only implemented the $\phi \rightarrow \gamma\gamma$ vertex for both mesons. As a result, the width for each meson in the simulation is different than the actual width. For π^0 , this difference is small since it decays to two photons the vast majority of the time. However, for η `CalcHEP` uses a width of 520 eV, whereas the actual width is approximately 1.3 keV [15].

Since the propagator of an unstable particle depends on the total width of the particle [28], the widths of the decays to photons as computed by `CalcHEP` are different than the actual widths. However, figure 3.8 shows a comparison between the off-shell case computed by `CalcHEP` and the on-shell case. The on-shell case does not depend on the total width of the meson. We see that regardless of the incomplete width used by `CalcHEP`, these values match closely.

4. Summary and Outlook

In this thesis, we have seen how introducing a new baryon number violating operator induces neutron decay to a proposed dark matter particle and a π^0 meson, η meson or photon. We have

found analytical expressions for the widths of these two-body decays as functions of the two free parameters of the theory: the mass of the dark fermion and the new physics scale.

Large mass experiments have put strict experimental constraints on exotic neutron decays, and consequently on the new physics scale for this theory. However, the neutrons in these experiments are generally bound, meaning that decays with a small mass gap cannot occur. We have therefore also analyzed the case of a small mass gap, where the new physics scale is the only free parameter in the theory.

The neutron decay to mesons was implemented in `CalcHEP` via an effective vertex. The meson decay to photons was also implemented, allowing for a Monte Carlo simulation of the $n \rightarrow X + \gamma\gamma$ decay. The width of this decay closely matches that of the decay where the meson is created on-shell, due to the narrow width of the mesons. This was also seen by an invariant mass reconstruction of the photons in this decay. This channel is a candidate for observation, as the resulting photons are relatively high energy. When the two photons are detected, an invariant mass reconstruction can be performed to determine the meson from which they originate. The dark fermion would show up as missing energy in the detector.

The upcoming HIBEAM and NNBAR experiments at ESS handle a large amount of free neutrons, and could therefore observe exotic neutron decays with a small mass gap. To test the applicability of this model to the HIBEAM and NNBAR experiments further, one could see how the new physics scale is constrained by past neutron experiments which are sensitive to small mass gap decays, and how the amount of expected neutrons at HIBEAM/NNBAR compares to this.

The operator considered has not been exhausted in this thesis. For example, the mesons can also decay to leptons or other mesons. Additionally, it is easy to imagine other BSM operators that would induce exotic neutron decays at small mass gaps, such as operators that violate quark family number, lepton number or operators that have different chiral structures. Furthermore, the case of a bosonic dark matter particle can also be considered. To investigate the possibility of observing exotic neutron decays at HIBEAM/NNBAR, one must enumerate these operators and the decays they induce as well as investigate the ability to observe the decay products in the detector with e.g. detector simulations.

This thesis has illustrated how such investigations can be done for one specific model, as well as the implementation of such models in `CalcHEP` which can generate events for detector simulation. With this, we hope to provide a source for future research on the possibility of observing rare neutron decays at the HIBEAM and NNBAR experiments.

Appendices

A. CalcHEP tables

vars.mdl

Name	Value	Comment
mx	0.2	Dark fermion mass
cutoff	1000000000000000	Interaction scale
D	0.8	Lattice Parameter
F	0.47	Lattice Parameter
beta	0.012	Lattice Parameter
fpi	0.0921	Pion decay constant
mn	0.9395654	Neutron mass
meta	0.54786	Eta mass
mpi0	0.13498	Pi0 mass
alpha	0.00729735252	fine structure constant
Pi	3.14159265358	

func.mdl

Name	Expression
c1	$\text{pow}(\text{cutoff}, -2)$
cnpi0	$-(D+F)/(2*fpi)$
cneta	$(-D+3*F)/(2*\text{sqrt}(3)*fpi)$
cmix	$\text{beta}*c1$
cxpi0	$\text{beta}*c1/(2*fpi)$
cxeta	$-\text{beta}*c1*\text{sqrt}(3)/(2*fpi)$
mnmxin	$1/(\text{pow}(\text{mx}, 2) - \text{pow}(\text{mn}, 2))$

prtcls.mdl (Columns number, width, color, LaTeX(A) and LaTeX(A+) are omitted.)

Full name	A	A+	2*spin	mass	aux
x	x	X	1	mx	0
neutron	n	N	1	mn	0
eta	eta	eta	0	meta	0
pi0	pi0	pi0	0	mpi0	0
photon	A	A	2	0	G

lgrng.mdl (Column P4 is omitted.)

P1	P2	P3	Factor	Lorentz Part
x	n	pi0	$i/2$	$\text{cxpi0}*(1+G5) + \text{cmix}*c\text{np}\text{i0}*m\text{nm}\text{x}\text{i}\text{n}\text{v}*(1+G5)*(-G(\text{p1})+\text{mn})*G(\text{p3})*G5$
N	X	pi0	$i/2$	$-\text{cxpi0}*(1-G5) - \text{cmix}*c\text{np}\text{i0}*m\text{nm}\text{x}\text{i}\text{n}\text{v}*G5*G(\text{p3})*(G(\text{p2})+\text{mn})*(1-G5)$
x	n	eta	$i/2$	$\text{cxeta}*(1+G5) + \text{cmix}*c\text{ne}\text{t}\text{a}*m\text{nm}\text{x}\text{i}\text{n}\text{v}*(1+G5)*(-G(\text{p1})+\text{mn})*G(\text{p3})*G5$
N	X	eta	$i/2$	$-\text{cxeta}*(1-G5) - \text{cmix}*c\text{ne}\text{t}\text{a}*m\text{nm}\text{x}\text{i}\text{n}\text{v}*G5*G(\text{p3})*(G(\text{p2})+\text{mn})*(1-G5)$
pi0	A	A	$\text{alpha}/(\text{Pi}*f\text{p}\text{i})$	$\text{eps}(\text{p2}, \text{m2}, \text{p3}, \text{m3})$
eta	A	A	$\text{alpha}/(\text{Pi}*f\text{p}\text{i})$	$\text{eps}(\text{p2}, \text{m2}, \text{p3}, \text{m3})$
N	n	pi0	$-i*c\text{np}\text{i0}$	$G(\text{p3})*G5$
N	n	eta	$-i*c\text{ne}\text{t}\text{a}$	$G(\text{p3})*G5$

B. FeynCalc input for trace evaluation

```
In[1]:= (*Import FeynCalc*)
<< FeynCalc`
FeynCalc 10.0.0 (stable version). For help, use the
online documentation , check out the wiki or visit the forum .

Please check our FAQ
for answers to some common FeynCalc questions and have a look at the supplied examples .

If you use FeynCalc in your research , please
evaluate FeynCalcHowToCite [] to learn how to cite this software .

Please keep in mind that the proper academic attribution
of our work is crucial to ensure the future development of this package !
```

Spin sum for the meson decay channels

```
In[2]:= (*Four-momentum conservation relations
used for simplification of the final expression*)
ScalarProduct [Subscript [p, n], Subscript [p, X]] =
(Subscript [m, n]^2 + Subscript [m, X]^2 - Subscript [m, ϕ]^2) / 2
ScalarProduct [Subscript [p, X], Subscript [p, ϕ]] =
(Subscript [m, n]^2 - Subscript [m, X]^2 - Subscript [m, ϕ]^2) / 2
ScalarProduct [Subscript [p, n], Subscript [p, ϕ]] =
(Subscript [m, n]^2 - Subscript [m, X]^2 + Subscript [m, ϕ]^2) / 2
ScalarProduct [Subscript [p, n], Subscript [p, n]] = Subscript [m, n]^2
ScalarProduct [Subscript [p, X], Subscript [p, X]] = Subscript [m, X]^2
ScalarProduct [Subscript [p, ϕ], Subscript [p, ϕ]] = Subscript [m, ϕ]^2

Out[2]=  $\frac{1}{2} (m_n^2 + m_X^2 - m_\phi^2)$ 

Out[3]=  $\frac{1}{2} (m_n^2 - m_X^2 - m_\phi^2)$ 

Out[4]=  $\frac{1}{2} (m_n^2 - m_X^2 + m_\phi^2)$ 

Out[5]=  $m_n^2$ 

Out[6]=  $m_X^2$ 

Out[7]=  $m_\phi^2$ 
```

In[11]:= (* Spin sum of n→phi+X *)

```
Simplify[TR[(- I Subscript[C, X ϕ] (1 + GA[5]) / 2 +
  I Subscript[C, mix] × Subscript[C, n ϕ] / (2 Subscript[m, X]^2 - 2 Subscript[m, n]^2)
  (1 + GA[5]).(GS[Subscript[p, X]] + Subscript[m, n]).GS[Subscript[p, ϕ]].GA[5]).
(GS[Subscript[p, n]] + Subscript[m, n]).
(I Subscript[C, X ϕ] (1 - GA[5]) / 2 +
  I Subscript[C, mix] × Subscript[C, n ϕ] / (2 Subscript[m, X]^2 - 2 Subscript[m, n]^2) ×
  GA[5].GS[Subscript[p, ϕ]].(GS[Subscript[p, X]] + Subscript[m, n]).(1 - GA[5])).
(GS[Subscript[p, X]] + Subscript[m, X])
]]
```

$$\text{Out[11]= } \frac{1}{(m_n^2 - m_X^2)^2} \left(-2 C_{\text{mix}} C_{n\phi} C_{X\phi} \left(-m_n^4 (3 m_X^2 + m_\phi^2) + 3 m_n^2 m_X^4 + m_n^6 + m_X^4 m_\phi^2 - m_X^6 \right) + \right. \\ \left. C_{\text{mix}}^2 C_{n\phi}^2 \left(-m_n^4 (m_X^2 + m_\phi^2) - m_n^2 (6 m_X^2 m_\phi^2 + m_X^4) + m_n^6 - m_X^4 m_\phi^2 + m_X^6 \right) + C_{X\phi}^2 (m_n^2 - m_X^2)^2 (m_n^2 + m_X^2 - m_\phi^2) \right)$$

Spin sum for the photon decay channel

In[17]:= (*Four-momentum conservation relations

used for simplification of the final expression*)

ScalarProduct[q, q] = 0

ScalarProduct[Subscript[p, n], Subscript[p, n]] = Subscript[m, n]^2

ScalarProduct[Subscript[p, X], Subscript[p, X]] = Subscript[m, X]^2

ScalarProduct[q, Subscript[p, n]] =

ScalarProduct[q, Subscript[p, X]] = (Subscript[m, n]^2 - Subscript[m, X]^2) / 2

ScalarProduct[Subscript[p, n], Subscript[p, X]] = (Subscript[m, n]^2 + Subscript[m, X]^2) / 2

Out[17]= 0

Out[18]= m_n^2

Out[19]= m_X^2

Out[20]= $\frac{1}{2} (m_n^2 - m_X^2)$

Out[21]= $\frac{1}{2} (m_n^2 + m_X^2)$

(* Spin sum of n→photon+X *)

```

In[24]:= Simplify[-(Subscript[C, mix]^2 * Subscript[C, ny]^2 * Subscript[F, 2]^2) /
  ((Subscript[m, X]^2 - Subscript[m, n]^2)^2) *
  TR[
    (I (1 + GA[5]).(GS[Subscript[p, X]] + Subscript[m, n]).DiracSigma[GA[beta], GA[v]].FV[q, v] / 2).
    (GS[Subscript[p, n]] + Subscript[m, n]).
    (-I .DiracSigma[GA[beta], GA[mu]].FV[q, mu].(GS[Subscript[p, X]] + Subscript[m, n]).(1 - GA[5]) /
    2).(GS[Subscript[p, X]] + Subscript[m, X])
  ]
Out[24]= 2 F2^2 Cmix^2 Cny^2 (m_n^2 + m_X^2)

```

Bibliography

1. Sakharov, A. D. Violation of CP Invariance, C asymmetry, and baryon asymmetry of the universe. *Pisma Zh. Eksp. Teor. Fiz.* **5**, 32–35 (1967).
2. Babu, K. S. *et al.* Baryon Number Violation 2013. arXiv: 1311.5285 [hep-ph].
3. 't Hooft, G. Symmetry Breaking through Bell-Jackiw Anomalies. *Phys. Rev. Lett.* **37**, 8–11. <https://link.aps.org/doi/10.1103/PhysRevLett.37.8> (1 July 1976).
4. Fukugita, M. & Yanagida, T. Baryogenesis Without Grand Unification. *Phys. Lett. B* **174**, 45–47 (1986).
5. Gavela, M. B., Hernández, P., Orloff, J. & Pène, O. *Standard Model Baryogenesis* 1994. arXiv: hep-ph/9407403 [hep-ph].
6. Belyaev, A., Christensen, N. D. & Pukhov, A. CalcHEP 3.4 for collider physics within and beyond the Standard Model. *Computer Physics Communications* **184**, 1729–1769. ISSN: 0010-4655. <http://dx.doi.org/10.1016/j.cpc.2013.01.014> (July 2013).
7. Miura, M. Search for Nucleon Decay in Super-Kamiokande. *Nuclear and Particle Physics Proceedings* **273-275**. 37th International Conference on High Energy Physics (ICHEP), 516–521. ISSN: 2405-6014. <https://www.sciencedirect.com/science/article/pii/S2405601415005659> (2016).
8. Abi, B. *et al.* Deep Underground Neutrino Experiment (DUNE), Far Detector Technical Design Report, Volume I Introduction to DUNE. *JINST* **15**, T08008. arXiv: 2002.02967 [physics.ins-det] (2020).
9. Bian, J. *et al.* Hyper-Kamiokande Experiment: A Snowmass White Paper in Snowmass 2021 (Mar. 2022). arXiv: 2203.02029 [hep-ex].
10. Santoro, V. *et al.* The HIBEAM program: search for neutron oscillations at the ESS. arXiv: 2311.08326 [physics.ins-det] (Nov. 2023).
11. Backman, F. *et al.* The development of the NNBAR experiment. *JINST* **17**, P10046. arXiv: 2209.09011 [physics.ins-det] (2022).
12. Davoudiasl, H., Morrissey, D. E., Sigurdson, K. & Tulin, S. Unified Origin for Baryonic Visible Matter and Antibaryonic Dark Matter. *Physical Review Letters* **105**. ISSN: 1079-7114. <http://dx.doi.org/10.1103/PhysRevLett.105.211304> (Nov. 2010).
13. Davoudiasl, H. Nucleon Decay into a Dark Sector. *Physical Review Letters* **114**. ISSN: 1079-7114. <http://dx.doi.org/10.1103/PhysRevLett.114.051802> (Feb. 2015).
14. Claudson, M., Wise, M. B. & Hall, L. J. Chiral Lagrangian for Deep Mine Physics. *Nucl. Phys. B* **195**, 297–307 (1982).
15. Workman, R. L. *et al.* Review of Particle Physics. *PTEP* **2022**, 083C01 (2022).
16. Aoki, Y. *et al.* Proton lifetime bounds from chirally symmetric lattice QCD. *Physical Review D* **78**. ISSN: 1550-2368. <http://dx.doi.org/10.1103/PhysRevD.78.054505> (Sept. 2008).
17. Pich, A. Effective Field Theory with Nambu-Goldstone Modes (eds Davidson, S., Gambino, P., Laine, M., Neubert, M. & Salomon, C.) arXiv: 1804.05664 [hep-ph] (Apr. 2018).
18. Huang, T. & Wu, X.-G. Determination of the eta and eta' Mixing Angle from the Pseudoscalar Transition Form Factors. *Eur. Phys. J. C* **50**, 771–779. arXiv: hep-ph/0612007 (2007).
19. Bijnens, J., Bramon, A. & Cornet, F. Pseudoscalar Decays Into Photon-photon in Chiral Perturbation Theory. *Phys. Rev. Lett.* **61**, 1453 (1988).
20. Griffiths, D. *Introduction to Elementary Particles* (Wiley-VCH, 2008).
21. Halzen, F. & Martin, A. D. *Quarks and Leptons: An Introductory Course in Modern Particle Physics* (Wiley, 1984).
22. Agostinelli, S. *et al.* Geant4—a simulation toolkit. *Nuclear Instruments and Methods in Physics Research Section A: Accelerators, Spectrometers, Detectors and Associated Equipment* **506**, 250–303. ISSN: 0168-9002. <https://www.sciencedirect.com/science/article/pii/S0168900203013688> (2003).

23. Allison, J. *et al.* Geant4 developments and applications. *IEEE Transactions on Nuclear Science* **53**, 270–278 (2006).
24. Allison, J. *et al.* Recent developments in Geant4. *Nuclear Instruments and Methods in Physics Research Section A: Accelerators, Spectrometers, Detectors and Associated Equipment* **835**, 186–225. ISSN: 0168-9002. <https://www.sciencedirect.com/science/article/pii/S0168900216306957> (2016).
25. Mertig, R., Böhm, M. & Denner, A. FEYN CALC - Computer-algebraic calculation of Feynman amplitudes. *Computer Physics Communications* **64**, 345–359. ISSN: 0010-4655. <https://www.sciencedirect.com/science/article/pii/001046559190130D> (1991).
26. Shtabovenko, V., Mertig, R. & Orellana, F. New developments in FeynCalc 9.0. *Computer Physics Communications* **207**, 432–444. ISSN: 0010-4655. <http://dx.doi.org/10.1016/j.cpc.2016.06.008> (Oct. 2016).
27. Shtabovenko, V., Mertig, R. & Orellana, F. FeynCalc 9.3: New features and improvements. *Computer Physics Communications* **256**, 107478. ISSN: 0010-4655. <http://dx.doi.org/10.1016/j.cpc.2020.107478> (Nov. 2020).
28. Peskin, M. E. & Schroeder, D. V. *An Introduction to Quantum Field theory* (CRC Press, Taylor & Francis Group, 2018).